Propeller Analysis Using RANS/BEM Coupling Accounting for Blade Blockage

David Hally[1]

[1] Defence Research and Development Canada
PO Box 1012, Dartmouth, Nova Scotia, Canada B2Y 3Z7

ABSTRACT

A popular method for analyzing a propeller operating behind a ship is to couple a Reynolds-averaged Navier-Stokes (RANS) solution of the flow around the hull with a solution for the flow around the propeller calculated using the Boundary Element Method (BEM). In the RANS/BEM coupling procedure, it is important that both solvers agree on the upstream propeller induction. Failure to do so causes an under-prediction of the thrust and torque. A method of accounting for the blade blockage by adding source terms to the equation of continuity in the RANS solver is described. Estimates of the importance of the blade blockage effect are obtained by analyzing the propeller of the well-known KRISO container ship (KCS).

Keywords

Propellers, effective wake, RANS, BEM.

1 INTRODUCTION

Although full Reynolds-averaged Navier Stokes (RANS) solutions of a propeller operating behind a ship are becoming more and more common, coupling a RANS solver for the flow around the ship with a solver using the boundary element method (BEM) for the propeller is an attractive alternative since far less CPU time is required. In the coupling scheme, the influence of the propeller on the RANS solution is usually introduced via a force field mimicking the action of the propeller; the influence of the hull on the BEM solution is introduced via an inflow wake calculated from the RANS solution but from which the propeller induction calculated by the BEM solver has been subtracted. Several iterations of RANS and BEM solutions are made until the BEM inflow wake, usually called the effective wake, no longer changes significantly.

For this scheme to work well it is important for two reasons that the force field used by the RANS solver generates an accurate representation of the flow upstream of the propeller:

1. It is the effect of the propeller induction on the hull that is the direct cause of the propeller-hull interaction. Inaccuracy in the induction will lead to inaccuracy in the flow over the hull and therefore in the effective wake; these, in turn cause inaccuracies in the predicted resistance of the hull and the predicted characteristics of the propeller (thrust, torque, etc.).

2. Since the propeller induction included in the RANS wake is removed by subtracting from it the propeller induction calculated by the BEM solver, any mismatch between the propeller induction calculated by the RANS and BEM solvers will appear as a contribution to the effective wake.
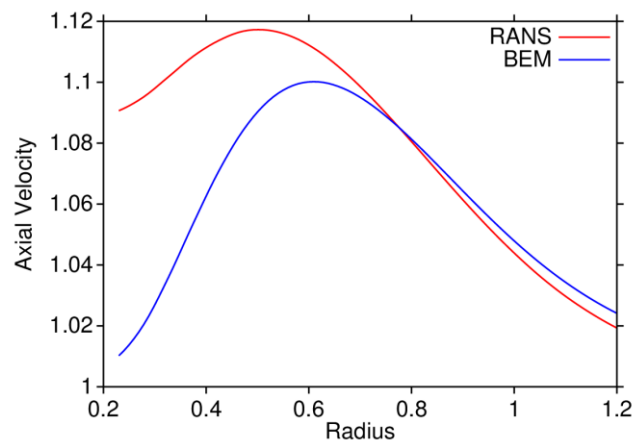

Figure 1: The induced axisymmetric axial velocity in a plane $0.3R$ upstream of the KCS propeller at $J = 0.7483$ in open water.

The match between the RANS and BEM induction velocities is easily checked using open water flow for which the effective wake is simply uniform inflow. However, when this is tried for a BEM solver which places the panels on the blade surfaces (rather than on the mean surface), the RANS axial induction velocities are always found to be larger than those of the BEM induction velocities (Fig. 1). The reason is that the physical bulk of the propeller blades retards the flow upstream; this blade blockage effect is included in the BEM solution but not in the RANS solution. Failure to account for blade blockage will cause the axial

velocity in the effective wake to be increased by the discrepancy effectively increasing the advance coefficient, *J*, and reducing the predicted thrust and torque.

Besides the numerical errors caused by the mismatch in induction, the blade blockage has physical effects. Since the induction is reduced, so is the thrust deduction. The difference between the nominal and effective wakes will also be somewhat smaller; since the effective wake is normally accelerated relative to the nominal wake, the blade blockage will tend to decrease the wake fraction, $1 - w$. For a fixed rotation rate, both effects lead to an increase of speed at the self-propulsion point; if the speed is held constant, both tend to decrease the rotation rate. Are these changes significant?

Hally and Laurens (1998) attempted to account for the blade blockage by calculating the flow within the blades in the BEM solver and using the pressure difference across the blade surface to adjust the force used in the RANS solver. Rijpkema et al. (2013) removed the blade blockage from the BEM induction by calculating it using only the dipole terms in the BEM solution; since they use BEM based on the Morino method (Morino and Kuo 1974), the blade blockage is represented by the source terms; however, this approach has the disadvantage that the induction is overestimated, so the difference between the nominal and effective wakes will also be overestimated. Therefore, while it reduces the numerical errors by avoiding the mismatch in the induction, it retains errors caused by the physical effects of an overestimated induction in the RANS solution.

This paper describes a third method: the blade blockage is included in the RANS solution by adding mass source terms to the equation of motion. Because the blockage is modelled in both RANS and BEM calculations, the numerical errors caused by a mismatch in induction are avoided and the physical effects of the blockage are taken into account. It has been implemented using the open source RANS solver OpenFOAM® and the BEM propeller code PROCAL developed by Cooperative Research Ships. PROCAL uses the Morino method (Morino and Kuo 1974) to calculate the velocity potential of the disturbed flow and has been validated extensively (Vaz and Bosschers 2006, Bosschers et al. 2008).

The new method has been used to investigate the importance of the blade blockage on the calculation of propeller performance.

2 RANS EQUATIONS WITH MASS SOURCES
When the blade blockage is modelled using mass source terms, the equations of motion to be solved by the RANS solver are

$$\frac{\partial v_i}{\partial x_i} = M, \qquad (1)$$

$$\frac{\partial v_i}{\partial t} + \frac{\partial (v_i v_j)}{\partial x_j} =$$
$$-\frac{1}{\rho}\frac{\partial p}{\partial x_i} + \frac{\partial}{\partial x_j}\left[\nu_t\left(\frac{\partial v_i}{\partial x_j} + \frac{\partial v_j}{\partial x_i}\right) + \delta_{ij}\frac{\partial v_k}{\partial x_k}\right] + F_i + M v_i \quad (2)$$

with implicit summation over repeated indices. The specific mass source density, M, and the force density, F_i, are determined from the BEM solution from the mass flux through each blade panel and the pressure on each blade panel respectively. The term proportional to M in the momentum equation (Eq. 2) arises when one puts the convective term in strong conservation form since the divergence of the velocity is no longer uniformly zero. To be completely consistent, one should add similar terms to the transport equations in the turbulence model. However, for the calculations described here, that was not done. Adding these terms would cause small changes to the flow downstream of the propeller; the change to the effective wake would be negligible.

Although, as indicated in Eq. 2, it is possible to use unsteady force and mass source fields in the RANS solver, the computational effort increases significantly. Since the main purpose for using the RANS/BEM coupling is to reduce the computation time, in the method described here the force and mass source fields are averaged in time. The RANS solution is then steady.

The RANS solver used in the method must allow source terms to be added to both the continuity equation and the momentum equations.

2.1 Calculation of the force and mass source densities
The calculation of the force and mass source densities is done in a cylindrical coordinate system, (x, r, θ), aligned with the propeller axis. The force density at a point within the volume swept out by the propeller is

$$\boldsymbol{F} = \sum_{f,b} \frac{Zp\hat{n}}{2\pi\rho r|\hat{\theta}\cdot\hat{n}|} \qquad (3)$$

where Z is the number of blades, p is the pressure on the blade as it passes through the point, $\hat{n}$ is the normal to the blade, ρ is the fluid density and $\hat{\theta}$ is a unit vector in the direction of rotation. The sum represents the fact that at each point one gets a contribution from both the face and the back of each blade. The dot product in the denominator is a geometric factor which accounts for the orientation of the blade normal to the direction of averaging ($\hat{\theta}$). Similarly, the specific mass source density is obtained from the mass flux through the blades by the inflow:

$$M = \sum_{f,b} \frac{-Z(\boldsymbol{V} + \omega r \hat{\theta}) \cdot \hat{n}}{2\pi r |\hat{\theta} \cdot \hat{n}|}$$

$$= \sum_{f,b} \frac{-Z\boldsymbol{V} \cdot \hat{n}}{2\pi r |\hat{\theta} \cdot \hat{n}|} + \frac{Z\omega}{2\pi} \sum_{f,b} \text{sgn}(\hat{\theta} \cdot \hat{n})$$

$$= \sum_{f,b} \frac{-Z\boldsymbol{V} \cdot \hat{n}}{2\pi r |\hat{\theta} \cdot \hat{n}|} \qquad (4)$$

Notice that the term in ω will vanish because the contribution from the face of the blade will exactly cancel the contribution from the back.

It is assumed that in the BEM solver the blades are covered by a mesh of quadrilateral panels which rotate through constant time steps. At each time step, the pressure at each panel corner point is known. As it rotates from one time step to the next, each panel sweeps out a hexahedral prism in the cylindrical coordinate space. The integrals of $\boldsymbol{F}$ and M over the hexahedron are easily calculated by constructing a trilinear interpolant between the values at the corner points. One obtains the force and volume rate associated with the hexahedron. Like the methods of force allocation described by Hally and Laurens (1998) and Rijpkema et al. (2013), each hexahedron is split into smaller hexahedra until the force and mass rate from each can be assigned to a cell in the RANS grid. The following algorithm is used:

1. Make a queue of all the hexahedra. The initial order of the hexahedra is not important.

2. Assign a split level of zero to each hexahedron.

3. Set a maximum allowed split level.

4. For each hexahedron, find the cells in the RANS grid which contain its corner points and store them with the hexahedron.

5. Repeat until the queue is empty:

   a. Remove the first hexahedron from the queue.

   b. If any two neighbouring corner points lie in different RANS cells that are not neighbours, then split the hexahedron in the direction of the edge, set the split level for each new hexahedron to the split level of the original hexahedron, and add the two hexahedra to the end of the queue. When the hexahedron is split, four new corner points are created; the RANS cells containing the corner points are found and stored with the new hexahedra.

   c. Otherwise, if all the corner points lie in the same RANS cell, calculate the force and volume rate for the hexahedron and assign them to that cell.

   d. Otherwise, if the split level is the maximum allowed, calculate the force and volume rate for the hexahedron then, for each corner point, assign one eighth of the force and volume rate to the RANS cell containing the corner.

   e. Otherwise, split the hexahedron along its longest edge, set the split level for the two new hexahedra to one more than the split level of the original hexahedron, and add the two hexahedra to the end of the queue.

6. For each cell in the RANS grid, divide the assigned force and volume rate by the volume of the cell to obtain a force density and specific mass density for the cell.

Step 4.b ensures that all the cells in the RANS grid which touch a hexahedron will be allocated a portion of its force and volume rate. Without this step, when the hexahedra are larger than the RANS cells (e.g. in the boundary layer of the shaft) it would be possible to miss RANS cells resulting in very uneven force and mass density fields.

Note, too, that the split level of a hexahedron is not increased until the criterion in 4.b. is satisfied; therefore the maximum split level is the number of times a hexahedron can be split once all its corner points lie in neighbouring cells in the RANS grid. A maximum split level of 3 provides a reasonable compromise between execution time and accuracy of the force and mass density distributions.

To implement this algorithm efficiently, it is essential that the search to find which cell in the RANS grid contains a corner point can be performed quickly. For this purpose the collection of RANS cells is first reduced to contain only those cells which intersect the swept volume of the blades. A hierarchy of bounding boxes for these cells is constructed. Each member of the hierarchy contains a range of cells, a bounding box for all the cells, and two pointers to lower branch of the hierarchy covering the first half of the range and the second half of the range. At the lowest level of the hierarchy, the range consists of a single cell. The cell containing a point is obtained by traversing the hierarchy to find a collection of cells whose bounding boxes contain the point (typically there will be only one or two of them), then querying those cells to determine which contains the point. The complexity of the search algorithm is $O(\log N)$ where N is the number of cells in the reduced set of RANS cells.

The full allocation algorithm requires that the following information be available from the RANS solver:

1. the number of cells in the RANS grid;

2. the volume of any cell;

3. a function to determine whether a point lies in a given cell;

4. a function that indicates whether a given pair of cells are neighbours; and

5. a bounding box for any cell (easily constructed from the corner points of the cell).

Each of these is available in the OpenFOAM mesh data structures.

2.2 Implementation in OpenFOAM

In the SIMPLE algorithm as implemented in OpenFOAM, the linearized discretized momentum equations are written in the form

$$AU = H - \nabla p \qquad (5)$$

Where U represents the velocity at each cell, A is a diagonal matrix and H includes all the off-diagonal terms not dependent on the pressure. This equation is used to obtain an expression for U,

$$U = A^{-1}H - A^{-1}\nabla p, \qquad (6)$$

the divergence of which provides an equation for the pressure, p:

$$\nabla \cdot (A^{-1}\nabla p) = \nabla \cdot (A^{-1}H) - M \qquad (7)$$

Therefore, in OpenFOAM, the source term $F_i + Mv_i$ must be added to the momentum equations and the source term $-M$ to the pressure equation.

To apply source terms in OpenFOAM one defines a class which applies the sources to the appropriate equations. Compiled code for the class is loaded at run-time. This mechanism has been used to implement the algorithm described in Sec. 2.1 and to apply the force and mass densities to the momentum and pressure equations. However, in OpenFOAM version 2.1 it is assumed that there will be no sources for the pressure equation so an additional modification is required to include them. Unfortunately, OpenFOAM contains many different solvers depending on the type of flow that is to be solved (steady, incompressible, with free surface, etc.) and each must be modified separately to include the mass density terms. To date, we have only modified `simpleFoam`, the solver for incompressible steady single-phase flows.

3 IMPLEMENTATION OF THE RANS/BEM COUPLING

The effective wake is the total wake in the propeller disk ($x = 0$) with the propeller induction subtracted from it. At iteration i of the RANS/BEM coupling, an approximation to the effective wake is given by

$$\begin{aligned} v^i_{\text{eff}}(r,\theta) &= v^{i-1}_{\text{RANS}}(0,r,\theta) \\ &\quad - \left(v^{i-1}_{\text{BEM}}(0,r,\theta) - v^{i-1}_{\text{eff}}(r,\theta) \right) \\ &= v^{i-1}_{\text{eff}}(r,\theta) + \Delta v(0,r,\theta) \end{aligned} \qquad (8)$$

where v_{RANS} is the total wake calculated by the RANS solver, v_{BEM} the total wake calculated by the BEM solver and Δv is their difference. The term in brackets is the induced velocity calculated by the BEM solver since $v^{i-1}_{\text{eff}}(r,\theta)$ is the wake in the propeller plane used as the inflow to the BEM solver on the previous iteration.

Because of the presence of the propeller blades, $v^{i-1}_{\text{BEM}}(x,r,\theta)$ is only available at points upstream of the propeller. To satisfy Eq. (8), values of Δv are extrapolated from upstream points to the propeller disk. The effective wake calculation is then:

1. Calculate the nominal wake, $v_{\text{n}}(x,r,\theta)$, using the RANS method.

2. Set $i = 0$ and the effective wake, $v^0_{\text{eff}}(r,\theta)$, to the nominal wake in the propeller disk.

   Repeat until the change in the effective wake is small enough:

   a. Run the BEM program with $v^i_{\text{eff}}(r,\theta)$ as inflow and use it to calculate the time averaged total wake $v^i_{\text{BEM}}(x,r,\theta)$.

   b. Calculate the time-averaged force and mass density fields implied by the BEM.

   c. Run the RANS solver with the force and mass density fields and use them to calculate the total wake, $v^i_{\text{RANS}}(x,r,\theta)$.

   d. Extrapolate $\Delta v(x,r,\theta)$ from upstream locations to the propeller plane.

   e. Calculate the effective wake using Eq. (8).

Different methods have been proposed for extrapolating Δv to the propeller plane. The simplest is to evaluate Δv in a plane just upstream of the propeller and assume that it will provide an adequate approximation of Δv at the propeller plane: that is, if the upstream plane is $x = x_1$, then

$$\Delta\mathbf{v}(0,r,\theta) = \Delta\mathbf{v}(x_1,r,\theta). \qquad (9)$$

Alternatively, one can evaluate Δv in two or more planes, then use a least squares linear fit for each of the values at constant (r,θ) to extrapolate to the propeller plane. If the upstream planes are $x = x_j$ for $j \in [1, N]$ then it is easy to show that the extrapolated values are then

$$\Delta\mathbf{v}(0,r,\theta) = \sum_{j=1}^{N} \alpha_j \Delta\mathbf{v}(x_j,r,\theta) \qquad (10)$$

with

$$\alpha_j = \frac{\overline{x^2} - \bar{x}x_j}{N(\overline{x^2} - \bar{x}^2)}; \quad \bar{x} = \frac{1}{N}\sum_{j=1}^{n} x_j; \quad \overline{x^2} = \frac{1}{N}\sum_{j=1}^{N} x_j^2 \qquad (11)$$

With two upstream planes this is equivalent to a linear extrapolation.

However, there is no reason that the upstream points need lie in planes and one can easily devise other methods: e.g. for each (r,θ) choose x so the point is a constant distance from the swept volume of the blades.

Which extrapolation method works the best in practice is a topic of on-going research. For the calculations described below, the simplest method was used: Δv was evaluated in a single upstream and the resulting value used in the propeller plane

It should be noted that this choice of extrapolation method is a conservative choice for the evaluation of the numerical

errors associated with the mismatch of the RANS and BEM induction. When blade blockage is ignored, the mismatch increases as one approaches the propeller. Linear or least squares extrapolation of Δv to the propeller plane will then tend to increase the mismatch causing larger errors.

4 KCS

In order to assess the importance of the blade blockage on predictions of propeller thrust and torque, the methods described in Secs. 2 and 3 were applied to the KRISO Container Ship (KCS), a test case that has often been reported in the scientific literature, in particular the 2000 and 2010 Gothenburg and 2005 Tokyo workshops on numerical ship hydrodynamics (Larrson et al., 2002, Larsson et al. 2013, Hino 2005). The KCS is a single screw container ship built only as a model. It is 7.2785m between perpendiculars, has a draft of 0.3418m and wetted surface area of $9.4389\,m^2$. It was equipped with a five-bladed propeller of moderate skew (24º at the tip) with diameter of 0.25m: see Fig. 2.
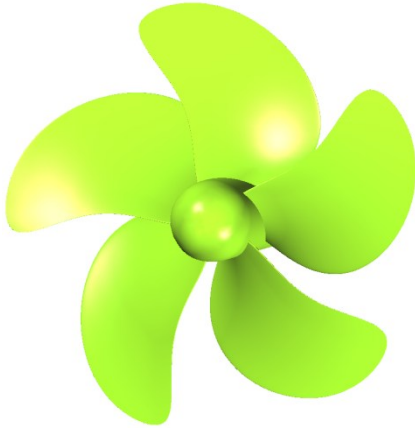

Figure 2: The KCS propeller.

The calculation was repeated three times:

1. with mass sources included in OpenFOAM; these calculation will be denoted "Blockage";

2. without mass sources and with the propeller induction calculated using only the BEM dipole source distribution as suggested by Rijpkema et al. (2013); these calculations will be denoted "No Blockage" and

3. without mass sources and with the propeller induction calculated using both the BEM sources and dipoles; these calculations will be denoted "Unmatched" since the RANS and BEM induction velocities will not match well.

Comparison of the first and second calculations provides an estimate of the importance of the physical effects of the blade blockage. Comparison of the first and third calculations provides an estimate of the errors incurred if the mismatch in RANS and BEM induction velocities is not accounted for.

The induction velocities were compared at the upstream plane at $x/R = 0.3$. Fig. 3 shows the location of the plane at $x = 0.3R$ relative to the swept volume of the blades and the hull centreplane. The velocities were compared on a grid of 21 radial points from $r/R = 0.19$ to 1.2 and 90 points around the circumference: 1890 points in all.
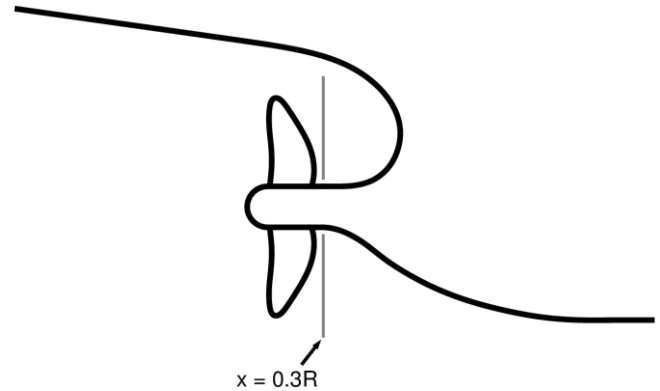

Figure 3: The location of the plane $x = 0.3R$.

After the nominal wake had been calculated, each calculation performed an additional four RANS/BEM coupling steps. The mean change in the effective wakes between the third and fourth iteration was less than $10^{-4}V$.

4.1 Calculation set-up

The OpenFOAM utility `snappyHexMesh` was used to generate a grid of 10 million cells with a mean y_+ value of 66. A refinement box was included upstream of the propeller disk above the shaft to ensure that the wake was adequately resolved.

For PROCAL, each side of each blade was covered with a 40×30 grid of panels (40 chordwise and 30 root to tip). A cylindrical hub was used extending $3R$ upstream and downstream. The locations of the wake panels shed from the trailing edges of the blades were prescribed according to empirical formulae for their pitch and radial contraction

The flow was calculated at a fixed draft of 0.3418 metres with no free surface. The Reynolds number based on the length between perpendiculars was $R_e = 1.4 \times 10^7$. To simplify the calculations, both the ship speed and the propeller rotation rate were fixed (at 2.196 m/sec and 9.5 revs/sec respectively). As the wave resistance was not calculated and the intent of the calculations was solely to determine the effect of the blade blockage, no attempt was made to determine the self-propulsion point.

4.2 Open water check of induced velocities

A check was made to ensure that the induction velocities calculated by PROCAL and OpenFOAM agreed well when the propeller was operating in open water with $J = 0.7483$,

the advance coefficient based on the average axial velocity in the "Blockage" effective wake field. The OpenFOAM induction was calculated both with mass sources and without. The PROCAL induction was calculated using both sources and dipoles (labelled BEM S+D) and using dipoles only labelled BEM D). Figs. 4 and 5 show comparisons of the axial and radial velocity components in the plane $0.3R$ upstream of the propeller plane. It can be seen that the RANS induction with mass sources agrees fairly well with the BEM induction with both sources and dipoles and that there is similar agreement between the RANS induction without mass sources and the BEM solution with only dipoles.
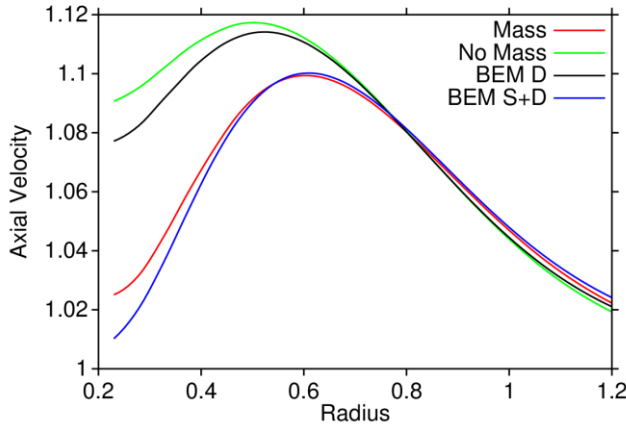

Figure 4: The induced axisymmetric axial velocity calculated by PROCAL and by OpenFOAM with and without mass sources.
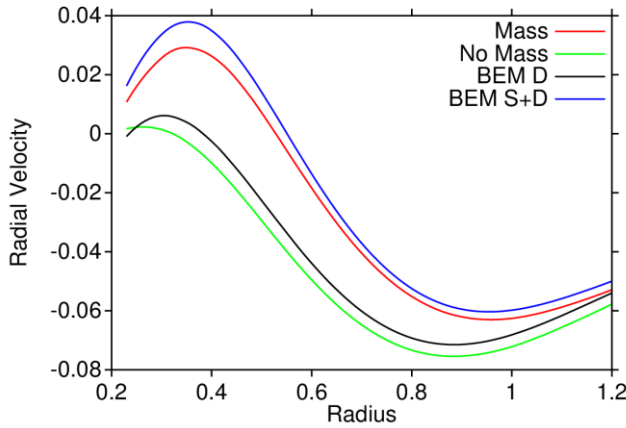

Figure 5: The induced axisymmetric radial velocity calculated by PROCAL and by OpenFOAM with and without mass sources.

4.3 Results

The nominal wakes from the experiment (Fujisawa et al. 2000) and the OpenFOAM calculation are shown in Figs. 6 and 7. The calculated wake is slightly deeper above the shaft and includes a pair of counter-rotating vortices

beneath the shaft that are not seen in the experiment. The tangential velocity components in the experiment are somewhat larger, likely due to the effect of the free surface.
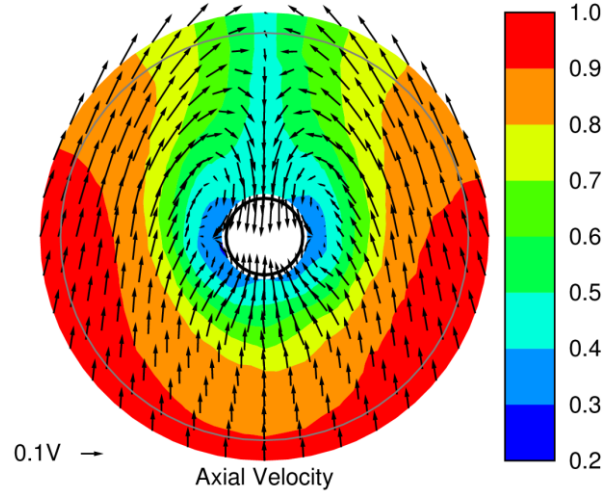

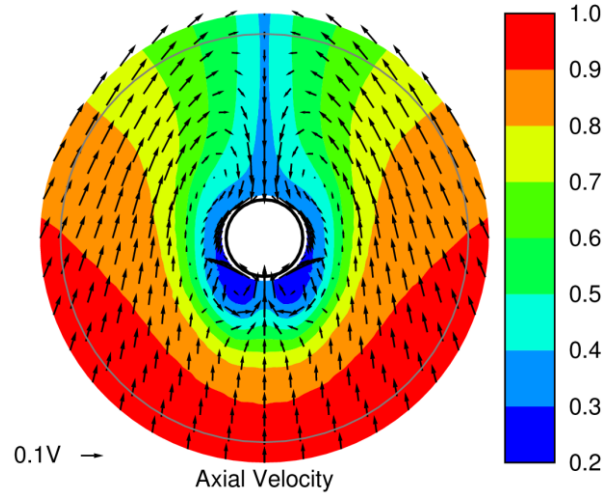**Figure 6:** The nominal wake measured at SRI.

Figure 7: The nominal wake predicted by OpenFOAM.

The "Blockage" effective wake calculated with mass sources is shown in Fig. 8. The effective wakes from the other two calculations are shown in Figs. 9 and 10 as differences from the wake in Fig. 8. Because the induction tends to cause a downstream axial acceleration, and since the BEM induction is larger when blockage is ignored, Fig. 9 shows an increase in the "No Blockage" axial velocities relative to the "Blockage" wake but it is small: the wake fraction $1 - w$ increases by only 0.2%. The maximum differences between the two wakes, about $0.016V$, occur near the locations of the vortices below and above the shaft in the nominal wake. The physical effects of the blade blockage cause only a small change to the effective wake.
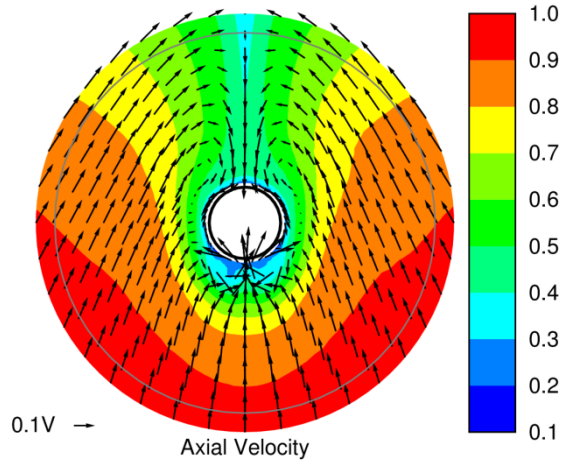
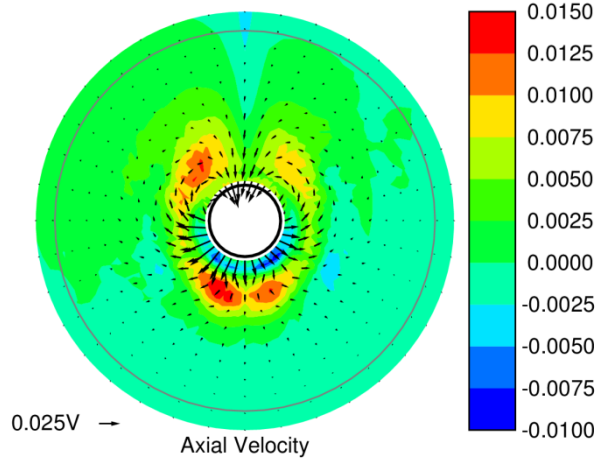**Figure 8:** The "Blockage" effective wake calculated with mass sources.

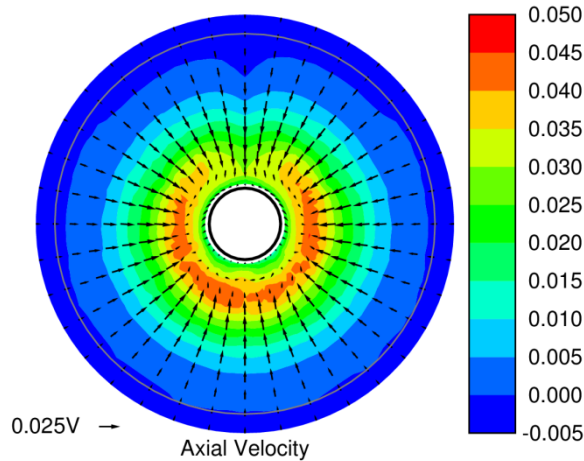**Figure 9:** The difference between the "No Blockage" and "Blockage" effective wakes.

Figure 10: The difference between the "Unmatched" and "Blockage" effective wakes.

The difference between the "Blockage" and "Unmatched" cases, shown in Fig. 10, is larger: the wake fraction $1 - w$ increases by about 1.6% with the maximum differences, about $0.045V$, occurring near $r = 0.4R$. The difference is clearly dominated by the near axisymmetric mismatch in the inductions which causes higher axial velocities and a net inward radial flow.

Table 1 lists the values of thrust coefficient, K_T, torque coefficient, K_Q, wake fraction, $1 - w$, viscous resistance coefficient, C_v, and pressure resistance coefficient, C_p, for each of the calculations. The percentages in the fourth and fifth columns show the change relative to the "Blockage" calculation.

Table 1: Calculated propulsion characteristics of the KCS propeller: fixed speed and propeller rotation rate; no free surface.

	Nominal	Blockage	No Blockage	Unmatched
K_T	0.2068	0.1946	0.1941 (-0.2%)	0.1890 (-2.9%)
$10K_Q$	0.3580	0.3393	0.3385 (-0.2%)	0.3316 (-2.3%)
$1 - w$	0.7178	0.7483	0.7496 (+0.2%)	0.7605 (+1.6%)
$1000C_v$	2.579	2.590	2.590 (0%)	2.590 (0%)
$1000C_p$	0.266	0.662	0.694 (+4.8%)	0.686 (+3.5%)

Because the effective wake is increased when the blade blockage is ignored, the thrust and torque decrease; however, provided that the mismatch in induction is accounted for, the decrease is small. On the other hand, if the induction mismatch is ignored, the decrease in thrust is comparatively large: about 3%. The decrease in torque is a little smaller.

While the propeller induction has a small effect on the viscous resistance (0.5%), the blade blockage causes no discernible change. Its effect on the pressure resistance, the principal component of the thrust deduction, is larger. When the blade blockage is ignored but the induction mismatch is not, the pressure resistance increases by 4.8% due to the higher induction velocities causing a larger pressure drop over the stern. When the induction mismatch is also ignored, the difference decreases to 3.3% because the increase in the effective wake causes the propeller thrust to decrease, in turn lowering the induction velocities and the pressure resistance. Relative to the total measured resistance at the self-propulsion point ($C_t = 3.534 \times 10^{-3}$ (Fujisawa

et al. 2000)) these represent changes of about 0.9% and 0.7% respectively; that is, failure to account for the blade blockage causes a change in the total resistance of a little less than 1% (it will be smaller at full scale).

If blade blockage is not accounted for, the increase in pressure resistance and the decrease in thrust combine to require an increase of thrust at the self-propulsion point: if the mismatch in induction is taken into account, the required increase is about 1.4%; if the mismatch in induction is ignored it is about 4%.

6 CONCLUSIONS

Failure to account for blade blockage when matching the RANS and BEM induction will lead to errors in ship powering predictions. The calculations described here suggest that, for typical single screw vessels, the physical effect of the blockage is to increase the thrust required at the self-propulsion point by the order of 1%. Most of this is due to an increase in the thrust deduction caused by the slower velocities upstream of the propeller caused by the blockage; a smaller part is caused by a small increase of the axial velocities in the effective wake causing the propeller to deliver less thrust.

When RANS/BEM coupling is used, the blade blockage also causes a mismatch in the induction velocities predicted by the RANS and BEM solvers since the blockage will be included in the BEM solution but not in the RANS solution. If this mismatch is not accounted for, the under-prediction of the required thrust at the self-propulsion point will be of the order of 4%. If linear or least squares extrapolation is used for Δv, this under-prediction will be larger (likely about 5%).

The mismatch in the RANS and BEM inductions can be corrected either by introducing the blockage into the RANS solution as described in Sec. 2 or by removing it from the BEM solution as in the method of Rijpkema et al. The former method has the advantage that the physical effects of the blockage are also included in the solution while they are ignored by the latter method. However, since the physical effects are small enough that they are very likely within the overall accuracy of the method, either method should give acceptable results.

REFERENCES

Bosschers, J., Vaz, G., Starke A.R., and van Wijngaarden, E. (2008). "Computational analysis of propeller sheet cavitation and propeller-ship interaction," Proc. of RINA MARINE CFD Conference CFD2008, Southampton, UK.

Hally, D., and Laurens J.-M. (1998). "Numerical Simulation of Hull-propeller Interaction Using Force Fields with Navier-Stokes Computations," Ship Technology Research, 45(1), 28-36.

Hino, T. (2005). Proc. of CFD Workshop Tokyo 2005, Tokyo, Japan.

Rijpkema, D., Starke, B., and Bosschers, J. (2013). "Numerical simulation of propeller-hill interaction and determination of the effective wake field using a hybrid RANS-BEM approach," Proc. 3rd International Symposium on Marine Propulsors, Launceston, Tasmania, Australia.

Fujisawa, J., Ukon, Y., Kume, K., and Takeshi, H. (2000), "Local Velocity Field Measurements Around the KCS Model (SRI M.S. No. 631) in the SRI 400m Towing Tank," SPD Report No. 00-003-2, Ship Research Institute, Ministry of Transport, Japan.

Larsson, L., Stern, F. and Bertram, V. (eds.), (2002). Gothenburg 2000, A Workshop on Numerical Ship Hydrodynamics, Chalmers University of Technology.

Larsson, L., Stern, F. and Visonneau, M. (eds.), (2013). Numerical Ship Hydrodynamics: An assessment of the Gothenburg 2010 workshop, Springer.

Morino, L. and Kuo, C.C. (1974). "Subsonic Potential Aerodynamics for complex configurations," AIAA Journal 12(2), 191-197.

Vaz, G. and Bosschers, J. (2006). "Modelling of three-dimensional sheet cavitation on marine propellers using a boundary element method," Proc. of 6th Inter. Symp. On Cavitation CAV2006, Wageningen, The Netherlands.